Anomalous Anomalies in Averaged Hydrographic Data*

M. SUSAN LOZIER

Ocean Sciences Program, Duke University, Durham, North Carolina

MICHAEL S. MCCARTNEY AND W. BRECHNER OWENS

Woods Hole Oceanographic Institution, Woods Hole, Massachusetts

ABSTRACT

A comparison of a recently assembled hydrographic database for the North Atlantic with the Levitus atlas shows striking differences in the vicinity of the Gulf Stream and the North Atlantic Current. On isopycnal surfaces in the main thermocline, isolated pools of warm, saline water are found in the Levitus database but are absent in the new database. Using synoptic data as a proxy for temporally averaged climatological data, it is shown that the anomalous features can be accounted for by the differences in the averaging process. To produce a gridded database from irregularly spaced station data, Levitus averaged the data on pressure surfaces while the new database was prepared with averaging on potential density surfaces. It is shown that averaging on a pressure surface in an area of sharply sloping isopycnals produces a water mass with a θ–S signature uncharacteristic of the local water mass(es). The anomalous potential temperatures and salinities that result are compared to the large-scale water mass anomalies of the North Atlantic and are shown to be of comparable strength. Finally, the consequences of having sizable averaging artifacts are discussed.

1. Introduction

It is generally recognized that a simple, but unfortunate, consequence of spatially smoothing hydrographic data is the broadening of property and dynamic fronts. Such broadening results regardless of whether the averaging is performed on a potential density, pressure, or neutral surface. Additionally, a second and perhaps more disconcerting consequence occurs with averaging on a pressure surface: a water mass is produced that has temperature–salinity characteristics dissimilar to those of the surrounding water. This dissimilarity results in temperature and salinity anomalies that are not due to *true* water mass variation, rather they are *artifacts* of the isobaric-averaging process. Thus, they are "anomalous anomalies." These anomalies were first noticed from a comparison of Levitus' (1982) hydrographic data with a hydrographic database recently completed for the North Atlantic (Lozier et al. 1994, hereafter LOC). From a collection of historical station data, mean water properties were determined for evenly spaced one-degree grid elements for

each database. Given the highly irregular distribution of station data such a determination necessitated a spatial averaging of the data. Levitus chose to average the data on surfaces of constant pressure, while LOC chose surfaces of constant potential density with varying reference pressures. Other differences between the databases are noteworthy. The Levitus atlas was prepared for the World Ocean; it is based on hydrographic data collected prior to 1976, and the scale of spatial smoothing is on the order of 1000 km. The LOC database is for the North Atlantic only; it uses all hydrographic data collected prior to May 1990, and its scale of spatial smoothing is on the order of 100 km. The notable increase in resolution was afforded by the high data density in the North Atlantic (relative to the other ocean basins) as well as by a marked increase in data density since 1976; the LOC database contains 60% more data than the Levitus database for the North Atlantic.

Because the Levitus atlas has become a widely used oceanographic reference, the LOC property fields were compared to the Levitus property fields (after a projection of the two databases onto common isopycnals). In general, for the upper and deep waters of the North Atlantic the overriding difference between property maps of the two databases is one of resolution. At middepths, however, comparisons yielded some unexpected results. To illustrate these results, properties on the surface, $\sigma_1 = 31.85$, are reproduced here. The Levitus mean pressure field (Fig. 1a) and the LOC mean

---

Corresponding author address: M. Susan Lozier, Department of Geology, Duke University, Old Chemistry Building, Durham, NC 27708-0230.

pressure field (Fig. 1b) exhibit differences that would be expected from the difference in the scale of smoothing: The Levitus pressure field has a considerably broader Gulf Stream, the curvature of the isobars at the Tail of the Grand Banks is virtually absent, and isobars for the Gulf Stream intersect, rather than skirt, the coast near Cape Hatteras. In short, the Levitus

pressure field looks like a smoothed version of the LOC pressure field. The Levitus potential temperature field (Fig. 1c), however, is not simply a smoothed version of the LOC potential temperature field (Fig. 1d). Although both temperature maps exhibit the familiar large-scale pattern of the middepth North Atlantic, with the warm, saline Mediterranean Water tongue extend-
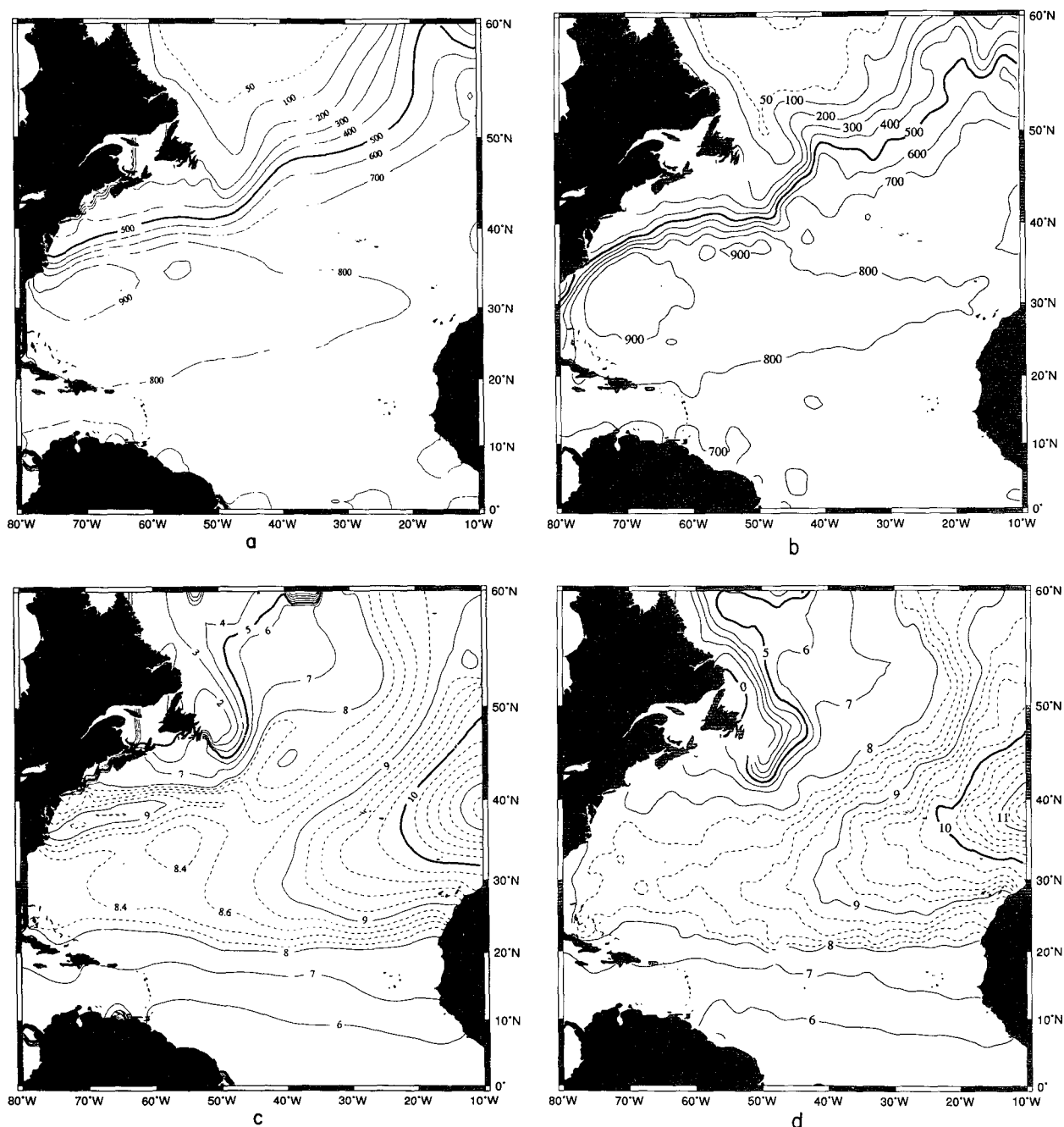

FIG. 1. (a) Pressure on the $\sigma_1 = 31.85$ surface from the Levitus database. (b) Same as for (a) but from the LOC database. (c) Potential temperature on the $\sigma_1 = 31.85$ surface from the Levitus database. (d) Same as for (c) but from the LOC database. For each plot the pressure units are decibars.

ing westward from the eastern boundary (splitting the colder, fresher waters from the South Atlantic and the Labrador Sea) and a sharp temperature gradient separating the warm Gulf Stream and the cold slope waters, there is a notable difference in these two fields. Prominent in the Levitus field but absent in the LOC field, is an isolated lozenge of warm water that extends along the mean path of the Gulf Stream from Cape Hatteras to approximately 60°W. The 9.0°–9.2°C water in this isolated lozenge contrasts sharply with the 8.2°C water found in the LOC field at the same locale. Not only is this water decidedly cooler, but there is no hint of closed isotherms in that vicinity for the LOC field. A difference is also found in the salinity field (not shown): a salty lozenge appears with salinities approximately 0.2 psu greater than those found in the LOC database. These potential temperature–salinity (hereafter θ–S) characteristics differ dramatically from those of the surrounding waters but are similar to those of the Mediterranean Water tongue east of the Mid-Atlantic Ridge along 38°W. Although this warm pool in the Levitus field closes near 60°W, a warm (8.2°C) tongue of water extends northeastward along the path of the Gulf Stream and the North Atlantic Current to approximately 50°N, 40°W. From this field it appears that a tongue of warm and saline Sargasso Sea water is carried northward along the axis of the North Atlantic Current. By contrast, the LOC field has isotherms (6°–7.2°C) paralleling isobars in this vicinity, indicating a North Atlantic Current that carries, on average, a monotonic gradient of water types from the cold and fresh "Mixed Waters" (Worthington 1976) inshore of the current to the subtropical waters on its offshore side.

These anomalously warm features in the Levitus field appear in isolation, surrounded by cooler waters. Thus, they cannot result from additional smoothing of the LOC database since smoothing does not create local extrema. This paper addresses the question as to what *does* cause these differences in the two databases. In the next section a simple model of isobaric averaging is presented to explain the anomalous features in averaged data. In section 3 the differences between isobaric and isopycnal averaging are identified and quantified. A discussion on the impact of averaging artifacts is provided in section 4, followed by conclusions in section 5.

2. A simple model of isobaric averaging

Since the difference in smoothing scales cannot produce the noted differences in the two databases, two other possible explanations will be examined. First, the distribution and/or characteristics of the hydrographic data collected from 1976 to 1990 might have significantly changed the mean temperature field in the vicinity of the Gulf Stream and the North Atlantic Current. This explanation is rejected because a map of the potential temperature field using the procedures of LOC with only the data collected prior to 1976 (not shown) does not contain any vestige of the warm lozenge seen in Fig. 1c. Second, averaging the data on isobars might produce a significantly different average than that produced by averaging on isopycnals. To examine this possibility it is necessary to isolate the effect of the averaging process from that of the smoothing scales. To achieve this, the LOC raw data was reaveraged on isobars with the same smoothing scheme and scales as applied to the LOC isopycnal-averaged data. The overall pattern and gradient strength of the potential temperature field (for the $\sigma_1 = 31.85$ surface) that resulted from this isobaric averaging (Fig. 2) closely resembles the LOC isopycnal-averaged field (Fig. 1d). However, an important difference is again observed in the vicinity of the Gulf Stream. For the isobaric-averaged field a large pool of 8.4°–8.5°C water extends from approximately 32° to 40°N, yet the isopycnal-averaged field has cooler waters (8.0°–8.4°C) and a monotonic gradient in that locale. The pattern of the feature in the isobaric-averaged field, with anomalously warm waters in the vicinity of the Gulf Stream, is similar to that for the Levitus field (Fig. 1c). The reduced magnitude of the anomalous waters (8.4°–8.5°C compared to 9.0°–9.2°C in the Levitus map) is due to reduced spatial smoothing for the LOC map, as will be discussed later. Finally, we note that the differences between the LOC isopycnal-averaged data fields and those obtained from isobaric averaging with the same LOC smoothing scales are significant enough to affect an interpretation of the flow at this depth. From the
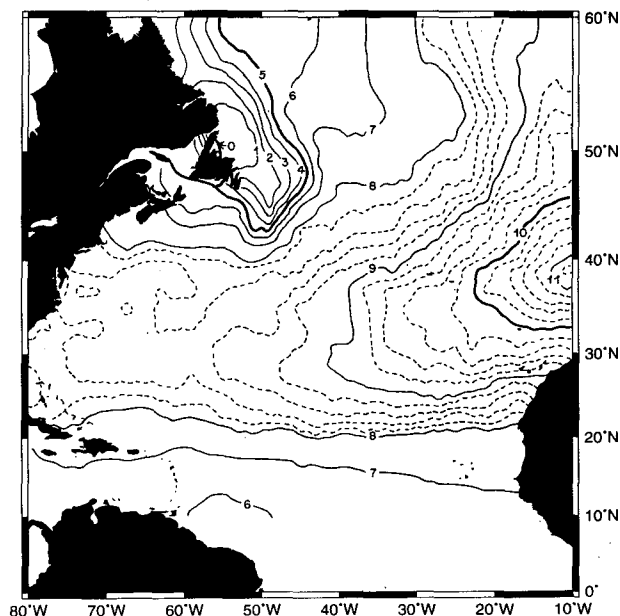

FIG. 2. Potential temperature (°C) on the $\sigma_1 = 31.85$ surface using isobaric-averaged data (from the LOC database) with the same smoothing scales as applied in Fig. 1d.

isobaric-averaged field one might interpret that the Mediterranean Water tongue turns northward west of Bermuda and penetrates the Gulf Stream system. By contrast, in the isopycnal-averaged field the Mediterranean Water tongue axis extends essentially westward at 28°N with a steady decrease in strength and no northward branch.

Since the only difference between the potential temperatures mapped in Figs. 1d and 2 is the averaging process, it is apparent that averaging on pressure surfaces in the vicinity of fronts produces mean potential temperatures (and salinities) that differ from those produced from averaging on potential density surfaces. A simple model of the Gulf Stream provides an explanation for this difference. Consider a geographic point near the mean axis of the meandering Gulf Stream and make two simplifications of the real ocean. First, ignore the small difference in thermocline θ–S relationship between the Sargasso Sea and slope water sides of the stream and suppose the water has the standard θ–S relation (Worthington and Metcalf 1961; Iselin 1936) as quantified by Armi and Bray (1982). Thus, the Gulf Stream is simplistically considered to be a potential density front but not a water mass front. Second, suppose that the meandering amplitude of the Gulf Stream is sufficiently large such that it spends most of the time either north or south of the point in question. Thus, the mean properties for a given depth at that locale are simply averages of the properties north and south of the front. Due to the strongly sloping isotherms and isohalines defining the front the temperatures on an isobaric surface spanning the front can differ by as much as 10°–12°C and the salinities by as much as 1.0–1.2 psu.

From a synoptic hydrographic section along 53°W (Table 1), representative potential temperatures from north of the Gulf Stream front were averaged with representative potential temperatures from south of the front at four selected isobars: 400 db, 600 db, 800 db, and 1000 db. The salinities were similarly averaged. Superposed on the standard θ–S curve in Fig. 3 are the averages that result for the four depths. (For simplicity the average is assumed to fall midway on the mixing line connecting the two end members.) From this plot it is apparent that because of the curvature in the θ–S relation the linear averaging lines will not coincide with the standard curve. Thus, an averaged potential temperature and salinity will not lie on the property–property curve. For example, at 600 db (the mean pressure
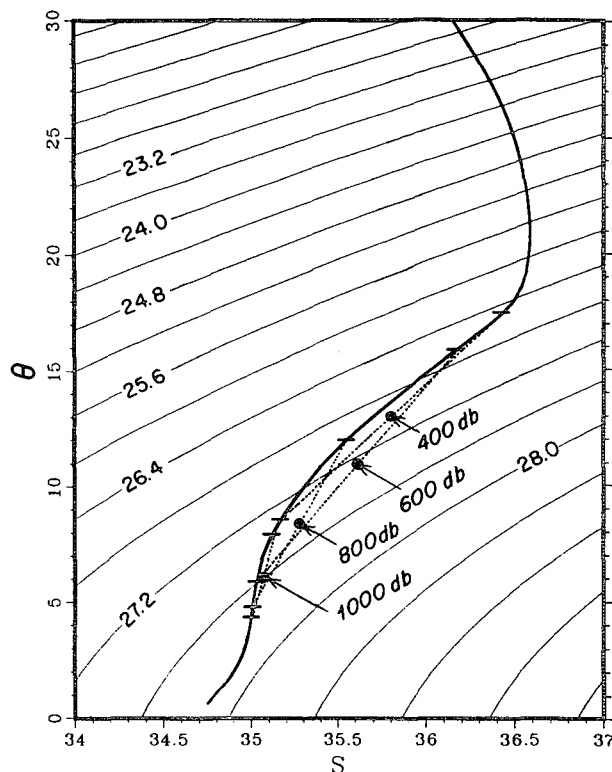

FIG. 3. A representation of the isobaric-averaging process using the standard θ–S relation for NACW. The mixing lines result from an average of temperatures and salinities north and south of the Gulf Stream front using data from the 53°W section. Averages at 400, 600, 800, and 1000 db are shown. The end-members for each of the selected isobars are marked by short horizontal bars and they are connected by a straight mixing line with the midpoint marked by a heavy dot. The background contours are lines of constant σ_θ.

of the isopycnal surface in Figs. 1a,b) the resulting average, 11°C and 35.6 psu, falls off the standard curve by an amount of 1.5°C (at a constant salinity) and 0.2 psu (at a constant potential temperature). Measured along an isopycnal (σ_θ) the differences are 2°C and 0.4 psu. These differences represent a water mass anomaly produced solely by isobaric averaging. Similar warm and salty anomalies appear at the other depths, although the magnitude of the averaging artifacts is smaller at 400 and 1000 db. This decrease is due to the reduced curvature in the θ–S relation at these depths. Thus, in a region of sloping isopycnals the averaging artifacts will be concentrated at thermocline

TABLE 1. Information on the synoptic sections used in the analyses of sections 2 and 3.

Section	Cruise	Date	Station spacing	Reference
Gulf Stream near 73°W	Endeavor 87	July 1982	~15 km	Johns et al. (1989)
Gulf Stream along 53°W	Oceanus 133	May 1983	~22 km	Knapp and Stommel (1985)
North Atlantic Current along 35°W	Knorr 104	August 1983	~50 km	McCartney (1992)

depths in the North Atlantic, where the curvature in the θ–S relation is greatest. Pressure averaging artifacts are also anticipated in regions such as the North Pacific and the Southern Ocean where low salinity intermediate waters create a pronounced salinity minimum (with an associated strong curvature in the θ–S relation) below the main thermocline.

The magnitude of this model-produced artifact is larger than the artifact noted in the Levitus field (Fig. 1c) because of the two simplifying assumptions of our model. First, intermediate temperatures within the stream would also be sampled in the real ocean, rather than just a temperature north and a temperature south of the stream. With these temperatures included, the average would fall between the standard curve and the straight line shown in Fig. 3. The line represents an upper bound on the possible size of the averaging artifact. Second, the θ–S relation is not constant in the real ocean and this simplification could, potentially, increase the magnitude of the averaging artifact. For example, the slope water relation tends to fall slightly on the fresh side of the Sargasso Sea relation, so that the cold end-member defining the line will be shifted to the left of the Sargasso curve, decreasing the upper bound on the anomaly set by the line. Finally, we note that the effect of isobaric averaging is reminiscent of the cabbeling process in which the mixing of two parcels of equal potential density produces a denser product because of the nonlinearity of the equation of state. While the cabbeling process is an element of the *real* physical mixing of the ocean, it is important to realize that the anomalous temperature and salinity properties seen in Fig. 3 are averaging *artifacts* and not genuine property anomalies.

From this simple analysis it is evident that there are two necessary conditions for an isobaric average to produce a spurious water mass: meandering of the sloped isopycnals of a front and curvature in the θ–S relation. The former limits the geographic locale where spurious water masses would be expected and the latter limits the artifacts to depths where the potential temperature and salinity relationship is nonlinear. Conversely, if averaging across the front is performed along an isopycnal, it will be shown that the averaged water mass will lie on the synoptic curve if there is one water mass present. If the front separates two (or more) water masses, the isopycnal-averaged θ–S characteristics will lie between the water masses in θ–S space, thus producing a realistic average. For the simple model discussed above, an isopycnal average lies exactly on the synoptic curve because there is no water mass variation across the front.

3. Isobaric versus isopycnal averaging

The above argument for the production of artifacts by the isobaric-averaging process is based on the temporal meandering of isotherms past a fixed locale. Both climatological databases (Levitus and LOC) are inherently smoothed by this temporal variability. Additionally, as noted earlier, the databases are spatially smoothed, the first over a scale of order 1000 km and the second over 100 km. To further identify and quantify differences in the averaging processes, temporal variability needs to be isolated from the spatial variation. To achieve this the property variation across a synoptic hydrographic section is used as a proxy for the temperature variability at a fixed locale in the vicinity of a meandering front (such as the Gulf Stream). In other words, we are assuming that a spatial average across a synoptic section, which cuts across a meandering density front, is roughly equivalent to a temporal average at a fixed locale within that front. Inherent in this choice is the assumption that the meandering envelope is on the order of the width of the current or larger. This assumption is supported by Fuglister's (1963) classic multiship survey of the Gulf Stream where the meridional width of the meander envelope was estimated to be 500 km, compared to a nominal stream width of 100 km. Such scales are also consistent with Cornillion's (1986) estimates based on satellite IR images.

Three synoptic sections from the North Atlantic are used as the proxies for our study: Two sections across the Gulf Stream are used, one near the point of the stream's separation from the western boundary (Endeavor 87, near 74°W) and the other west of the stream's bifurcation near the Grand Banks of Newfoundland (Oceanus 133 along 53°W). The third section crosses the North Atlantic Current (Knorr 104, along 35°W). For brevity we will refer to these lines as 74°W, 53°W, and 35°W. All three sections are vertically high-resolution (2 db) CTD data. Further particulars about these sections can be found in the references listed in Table 1.

a. Direct comparison of averaging processes

For a direct comparison of averaging processes, potential temperature and salinity from the 74°W section were interpolated onto selected isopycnals and isobars. These properties were then spatially averaged over a horizontal distance (200 km) set by the rise of the isopycnals, as shown in Fig. 4a. Three averages were made using this scale: 1) Temperatures and salinities were averaged along isobars spaced every 20 db. 2) Temperatures and salinities were averaged along isopycnals that coincided (on the offshore side of the front) with the isobars used for averaging. The potential temperatures and salinities were averaged along an isopycnal unless the isopycnal outcropped somewhere along the horizontal averaging width. In such a case, no average was made. 3) Temperatures and salinities were averaged along a neutral surface. As with the isopycnal averaging, neutral surfaces were traced across the section from points originally coincident with the selected iso-
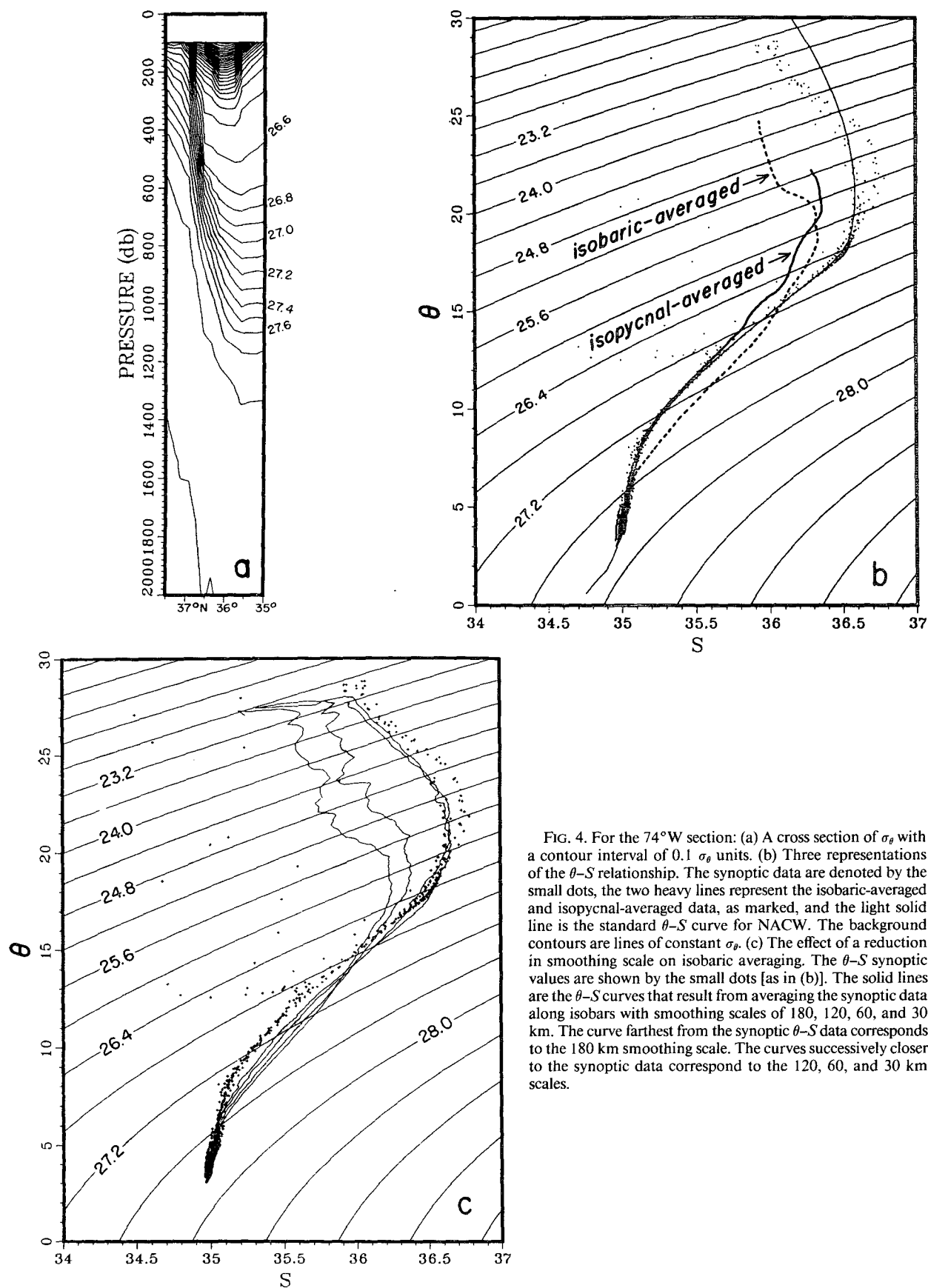
FIG. 4. For the 74°W section: (a) A cross section of σ_θ with a contour interval of 0.1 σ_θ units. (b) Three representations of the θ–S relationship. The synoptic data are denoted by the small dots, the two heavy lines represent the isobaric-averaged and isopycnal-averaged data, as marked, and the light solid line is the standard θ–S curve for NACW. The background contours are lines of constant σ_θ. (c) The effect of a reduction in smoothing scale on isobaric averaging. The θ–S synoptic values are shown by the small dots [as in (b)]. The solid lines are the θ–S curves that result from averaging the synoptic data along isobars with smoothing scales of 180, 120, 60, and 30 km. The curve farthest from the synoptic θ–S data corresponds to the 180 km smoothing scale. The curves successively closer to the synoptic data correspond to the 120, 60, and 30 km scales.

bars on the offshore side of the front. Additionally, potential temperatures and salinities were averaged along this surface unless it also outcropped. Because this latter averaging process produced mean temperatures and salinities that were indistinguishable from those produced via isopycnal averaging, our subsequent discussion will be restricted to isobaric and isopycnal averaging. The results from these two averaging processes are summarized in Fig. 4b. Superposed on the actual temperatures and salinities are the temperatures and salinities from the isobaric and isopycnal averaging. It is evident from Fig. 4b that the isopycnal-averaged values lie within the cloud of points designating the actual $\theta-S$ values. Below the $\sigma_\theta = 26.8$ surface the isopycnal-averaged values lie directly atop the actual values because of the tight synoptic $\theta-S$ relationship. On lighter surfaces the isopycnal-averaged $\theta-S$ values reflect a mix of North Atlantic Central Water (hereafter NACW) and the colder and fresher slope water. Finally, consistent with the simple model discussed in section 2, the isobaric averaging has created values warmer and saltier than either of the two water masses present and is largest where the curvature is the greatest. Furthermore, it is seen in Fig. 4b that the near-surface properties from the isobaric averaging are anomalously cool and fresh because of the negative curvature for waters warmer than approximately 20°C.

The fundamental difference between averaging along isobars or isopycnals is due to the differences in the property gradients along these two surfaces. For a strong dynamic front, temperature and salinity generally change more rapidly along an isobar than they do along an isopycnal. (In fact, if there is only one water mass present, there will be no change in temperature or salinity along an isopycnal.) Stating the problem in terms of gradients, it is apparent that the average will be sensitive to the scale of smoothing. To illustrate this dependence, potential temperature and salinity from the 74°W section were reaveraged using different scales of smoothing. The $\theta-S$ curves that result from smoothing these properties on scales of 180, 120, 60, and 30 km are shown in Fig. 4c. From this plot it is evident that as the smoothing scale is reduced the averaging process produces $\theta-S$ values closer to the true $\theta-S$ values. In other words, as the smoothing scale for a spatial average decreases, the line along which the averaging occurs shortens and converges to the $\theta-S$ curve. However, for the real ocean the reduction of the horizontal smoothing scale will not cause the isobaric average to converge to the isopycnal average, because the effect of temporal variability is irreducible. Regardless of whether there is *any* spatial smoothing, as long as there are sloping and meandering isotherms at a position, the difference in the averaging results will remain. Thus, even with a reduction in the spatial smoothing scale, an isobaric average still produces averaging artifacts, as evidenced in Fig. 2. To explain why the averaging artifacts are smaller in Fig. 2 than the anomalies found in the Lev-

itus field (when presumably the temporal variability is equivalent in both databases), we note that the Levitus spatial scale for smoothing exceeds the width of the meandering envelope. Thus, we presume that in addition to the anomalies created by the temporal variability, error is also introduced by the spatial smoothing. However, for the isobaric-averaged field shown in Fig. 2 (at a nominal resolution of 100 km), temporal variability is presumably the primary cause for the artifacts.

b. Quantification of averaging artifacts

To assess the impact of isobaric-averaging artifacts their relative magnitude needs to be determined. A criterion for the suitability of isobaric averaging should be whether or not the anomalies produced by this averaging are weak *relative* to those due to true water mass variations. Such a test has been made via the following steps:

1) Potential temperatures from the 53°W section were used to determine the corresponding salinities (S_{fit}) for characteristic NACW using the standard $\theta-S$ relation. The salinity anomalies ($S - S_{fit}$) that result are shown in Fig. 5a. (Note: to aid the interpretation of this plot and others in this series the reader is referred to Fig. 8a where the potential density is plotted.) This field of salinity anomalies is dominated in the south by fresh South Atlantic water (negative anomaly), which penetrates to approximately 23°N. The strong positive anomaly (salty) in the shallow waters south of 28°N is the salinity maximum water noted by Worthington (1976) that is formed in the upper 200 m by the excess of evaporation over precipitation in the Atlantic trade wind zone. The third anomaly of note is the Mediterranean Water anomaly, which lies below 800 m between 23° and 33°N. At 0.1 psu, this anomaly is weak this far west (53°W), relative to its strength at the Mediterranean outflow. Finally, the slope waters create a negative anomaly in the upper thermocline waters from 38°N to the section's end. A strong, fresh eddy centered at 600 m in the Gulf Stream is also seen in this section. Similar fresh eddies have been previously noted near this locale (McCartney et al. 1980).

2) Smoothed potential temperatures and salinities were computed at each station by averaging along an isopycnal all data within 100 km of the station. This smoothing scale was selected as a conservative estimate of the meandering envelope of the stream. From the smoothed potential temperature a salinity was determined using the standard $\theta-S$ relation. An anomaly was then computed by subtracting this fitted salinity value from the smoothed value ($\bar{S} - S_{fit\,from\,\bar{\theta}}$). In other words, if one had only smoothed data available, Fig. 5b is the anomaly plot that would result. The five anomalies noted in Fig. 5a are easily recognized in this smoothed version. Their location and maximum strength are preserved except for the small-scale eddy
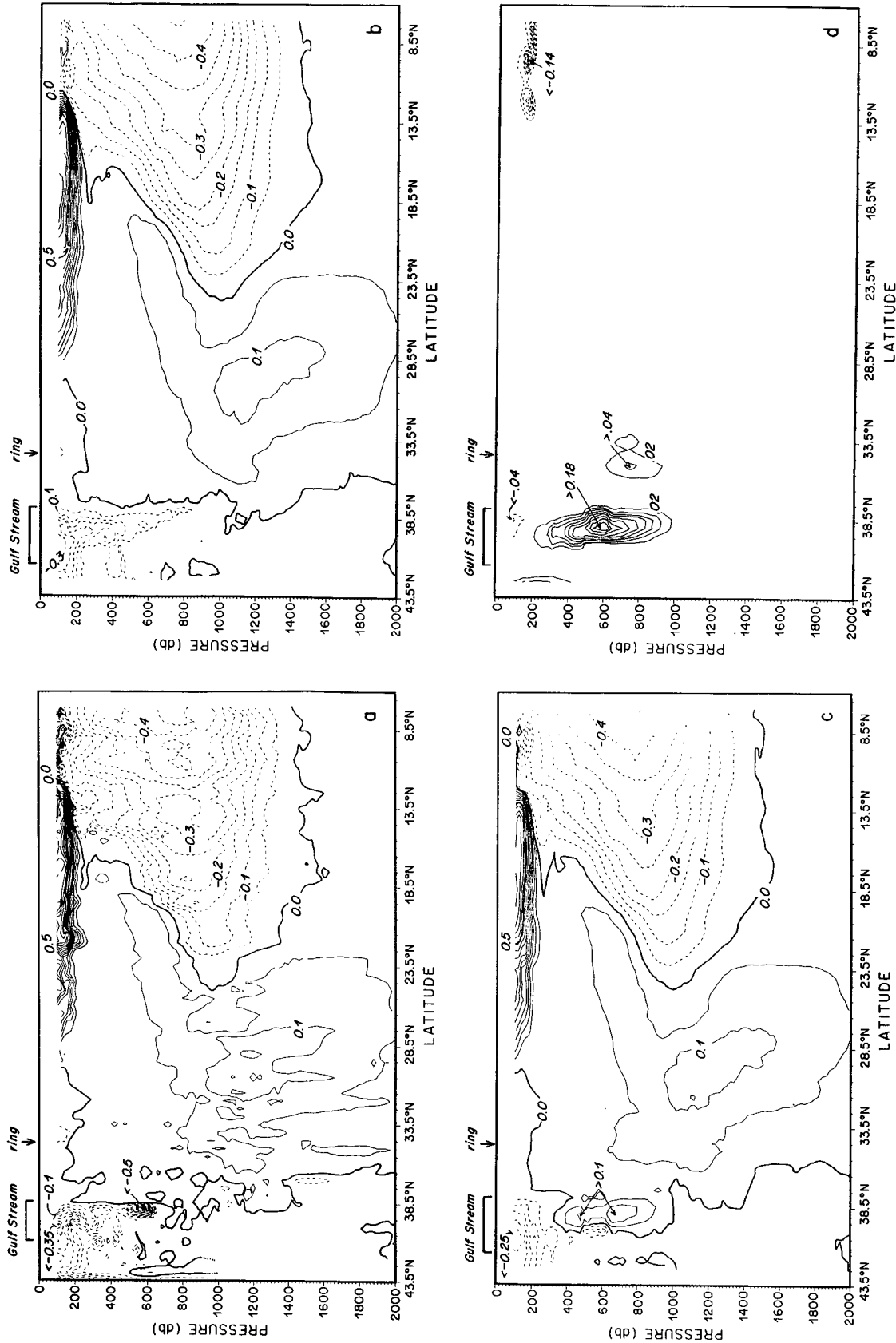
FIG. 5. Salinity anomalies for the 53°W section using the following: (a) unaveraged data, (b) isopycnic-averaged data, (c) isobaric-averaged data, and (d) isobaric-averaged data with only one water mass present (NACW). All contour intervals are 0.05 psu except for (d), where the contour interval is 0.02 psu and the zero contour is not included.

JOURNAL OF PHYSICAL OCEANOGRAPHY VOLUME 24

at the edge of the Gulf Stream. The smoothing has weakened its magnitude to the extent that it is no longer distinct from the slope water anomaly. In sum, isopycnal averaging has produced a smoothed version of the raw salinity anomaly plot.

3) The calculation in step 2 was repeated with the averaging performed on isobars. The South Atlantic water, Mediterranean tongue, and the salinity maximum water anomalies are all evident and apparently unchanged except for smoothing (Fig. 5c). A notable change though is the introduction of a positive (salty) anomaly centered on the Gulf Stream axis and extending from approximately 350 to 1050 m. This salty anomaly results strictly from isobaric averaging and is clearly an *anomalous anomaly*. It is the cross-sectional analog of the warm salty lozenge seen on the isopycnal surface earlier (Fig. 1c). The important result of this calculation is that the averaging anomaly is of comparable strength to the Mediterranean tongue (a *true* water mass anomaly). This signifies that averaging artifacts have the potential to affect interpretations of averaged data, as will be discussed in section 4.

4) To isolate the anomalies created from the averaging process from true water mass anomalies the calculations in steps 2 and 3 were repeated with a section that has no water mass variation. To accomplish this, standard salinities were determined from the section's potential temperatures using the standard θ–S relation. The two averaging procedures were then applied and anomalies for the smoothed salinities were then computed. From the anomaly plot for the isobaric averaging (Fig. 5d), it is evident that significant anomalies occur in the presence of sloping isopycnals. With the isolation of these anomalies from the true water mass anomalies, the fictitious Gulf Stream salty (and warm) lozenge is highlighted, and a weaker, warm anomaly, due to a cold core ring at 34°N, is also evident. Weakly negative (fresh) anomalies that appear in the upper waters of both the Gulf Stream and the North Equatorial Countercurrent are attributed to the negative curvature of the potential temperature–salinity relationship for the warm waters (Fig. 4b). For the same calculation using isopycnal-averaged data (not shown) no anomalies appear, because there is no water mass variation in this calculation. Averaging on an isopycnal *exactly* reproduces the true (synoptic) water mass characteristics because there are no temperature or salinity gradients along an isopycnal in this case.

From this analysis it is concluded that averaging on pressure surfaces produces anomalies comparable in magnitude to anomalies that represent true water mass variation. In the next section we will discuss the consequences of having the real and the "anomalous" anomalies the same order of magnitude.

4. Discussion

There is nothing inherently erroneous about averaging hydrographic data on pressure surfaces. Using an *x, y, p* Cartesian coordinate system, the average temperature or salinity at a point is well defined. As the Gulf Stream, for example, meanders latitudinally, a geographic locale will alternately lie in slope waters or Gulf Stream waters and its average temperature (for example) will simply lie between the temperatures of these two water masses. The problem we address in this paper lie not with this averaging process per se but rather with the interpretation and usage of the mean values produced by this averaging process. In this section we discuss the effect that spurious water masses might have on some of these usages. There is an important point to be made prior to this discussion: Averaged databases, in particular the Levitus atlas, have been and are of much value. The following discussion provides a cautionary note to users of such averaged databases and is not intended to dismiss the contribution of the atlas itself.

a. Interpretation of averaged hydrographic data

The most obvious impact of the spurious water masses will be on basic interpretations of charts and sections. For some presentations of data, anomalous water masses will clearly stand out, as is the case for the warm lozenge in Fig. 1c. Because the isolated feature in this map was inexplicable in terms of reasonable water mass variation, a data or data processing error was indicated. In other presentations, however, the artifact may not be so apparent. For instance, if the climatological mean potential temperature from the Levitus database is shown on an isobar (Fig. 6), rather than on an isopycnal (as in Fig. 1c), there is no apparent problem. In this presentation the anomaly created by isobaric averaging is masked by the strong background temperature gradient along the isobar. Thus, this presentation of the data, mapping on pressure surfaces, is perhaps the most damaging since the artifacts are more likely to go unnoticed. Similarly, climatological *mean* potential temperature or salinity sections (not shown) have no obvious problems; the averaging artifacts are revealed only by an examination of *anomaly* sections (like Fig. 5c).

Viewing data either on potential density surfaces or in terms of perturbation quantities (i.e., anomalies) provides the best chance to identify questionable data. However, in some cases the averaging process may yield subtle effects that are not as easily recognized as averaging artifacts even with such a presentation. The warm tongue along the North Atlantic Current in Fig. 1d and the bulge of warm water northward past Bermuda in Fig. 2 are examples of subtle averaging artifacts. Another example is illustrated by a series of salinity anomaly plots (Fig. 7), as calculated for the 53°W section in section 3b, but for the 35°W section, across the North Atlantic Current. To aid the interpretation of the salinity anomaly plots, potential density is shown in Fig. 7e. The series of rising isopycnals across this
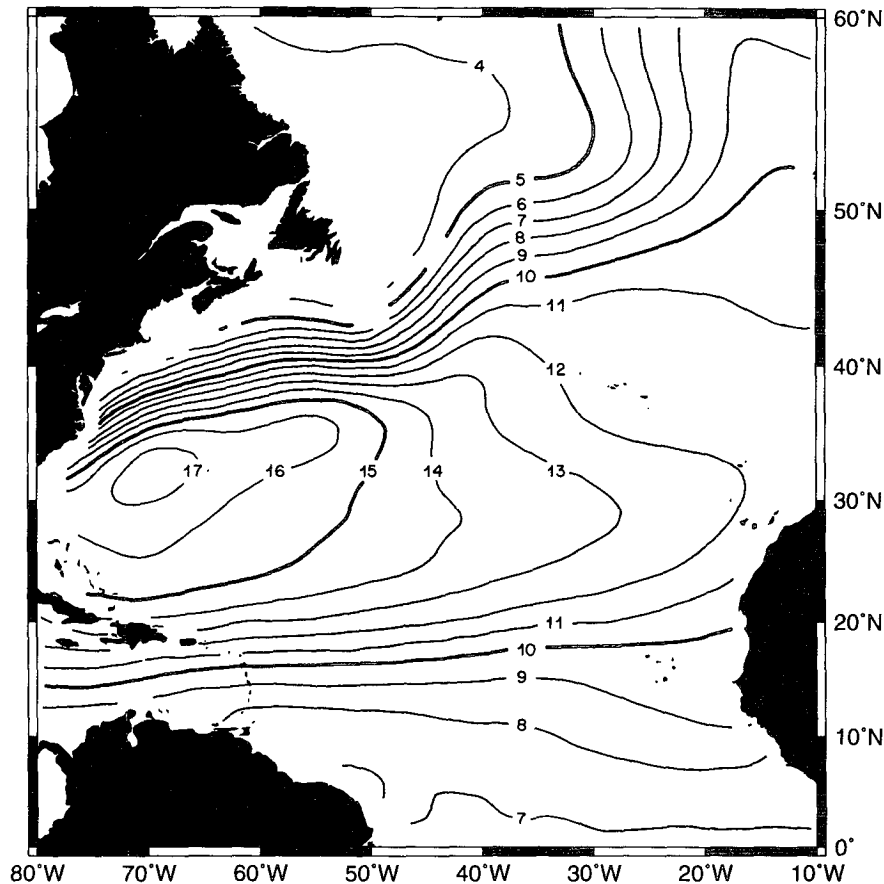
FIG. 6. A plot of potential temperature (°C) on the 500-db surface using the Levitus data.

section is a reflection of the strong meandering of the North Atlantic Current at the time of this observation. The unaveraged salinity anomaly plot (from step 1 in section 3b) shows a demarcation at 43°N between the salty waters of subtropical origin and the fresh waters of subpolar origin (Fig. 7a). When this plot is remade using data smoothed on potential density surfaces (as in step 2) the location of the front is broadened but remains at 43°N (Fig. 7b). However, the plot (Fig. 7c) produced by isobaric averaging (as in step 3) shows the front between these two water masses to be 5° farther north, at approximately 48°N. It is evident from Fig. 7d (produced as in step 4) that the shifting of this water mass boundary is due to the introduction of positive anomalies north of 43°N by isobaric averaging. The three bull's eyes in this figure correspond to the three regions of rising isopycnals in this section (Fig. 7e), with the strength of the averaging artifacts proportional to the slope of the isopycnals. In this case the anomalies produced via isobaric averaging are of the same order of magnitude as the salinity differences between the waters of subtropical and subpolar origins. Thus, they considerably degrade the estimation of the northern penetration of subtropical water.

In addition to the interpretation of maps or sections of water mass properties, hydrographic data are used in the determination of geostrophic shear. Given that anomalies are found in the isobaric-averaged temperatures and salinities, it is obvious to ask if such averaging affects the calculated shear. Since shear is approximately proportional to the horizontal gradient of the locally referenced potential density, we will examine the effect on shear by examining sections of potential density. Potential temperatures, salinities, and pressures from the 53°W section across the Gulf Stream were smoothed with both averaging schemes so that the unaveraged data at each station, θ, S, and P, were replaced with $\bar{\theta}$, $\bar{S}$, and $\bar{P}$. These smoothed properties were then used to calculate the potential density fields shown in Figs. 8b,c. Compared to the unaveraged potential density field (Fig. 8a), both averaged fields, which are visually comparable, show the familiar effect of the smearing of the width of the current. (Only an averaging scheme using streamwise coordinates would escape this broadening.) Away from the center of the Gulf Stream the isopycnals for the two fields are coincident, implying that the total geostrophic transports for the two averaged fields would be the same. However,
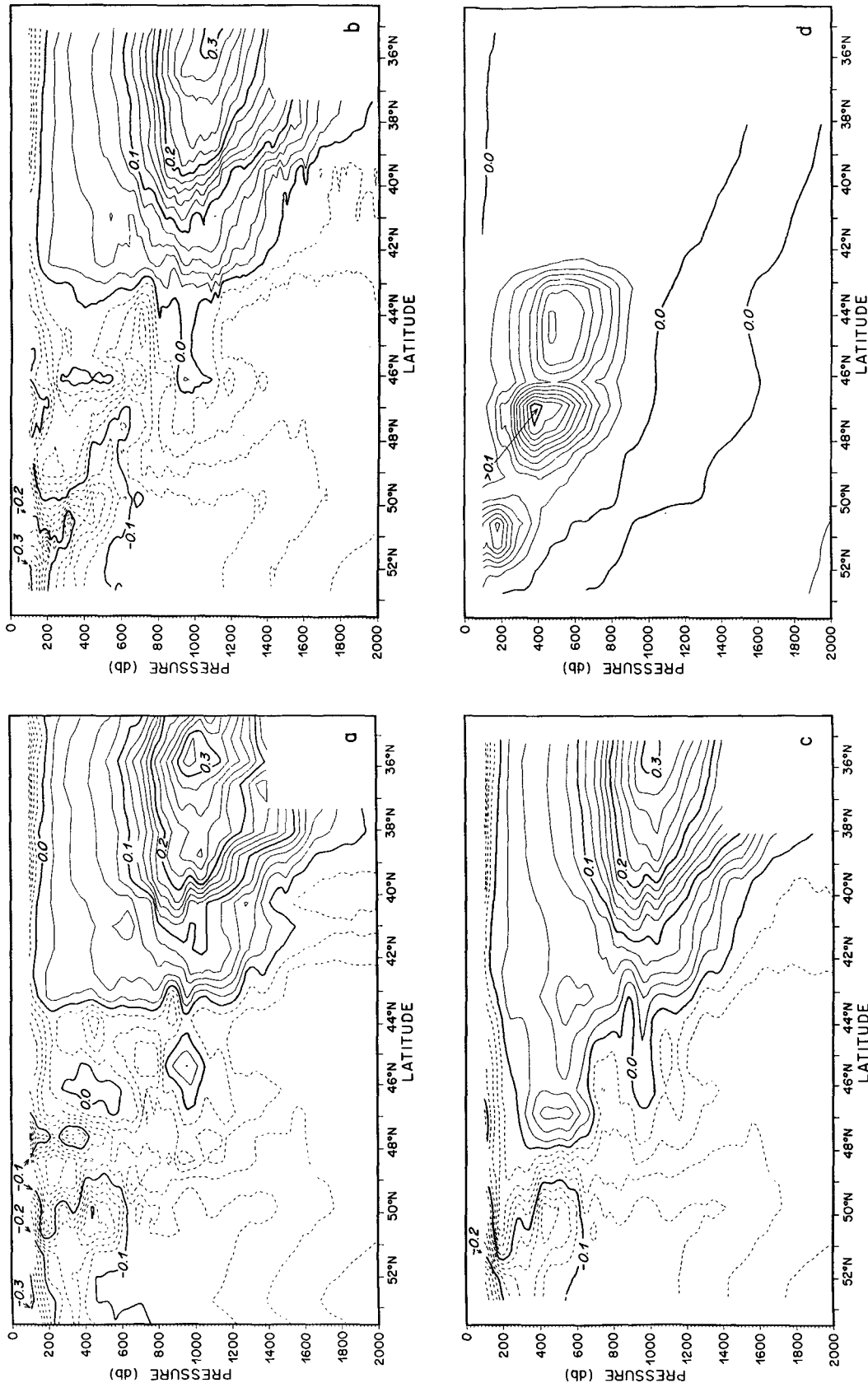
FIG. 7. Salinity anomalies for the 35°W section using (a) unaveraged data, (b) isopycnal-averaged data, (c) isobaric-averaged data, and (d) isobaric-averaged data using only NACW properties. (e) Potential density for the 35°W section. Contour interval is 0.1 σ_θ units. All contour intervals are 0.02 psu except for (d), where the contour interval is 0.01 psu.
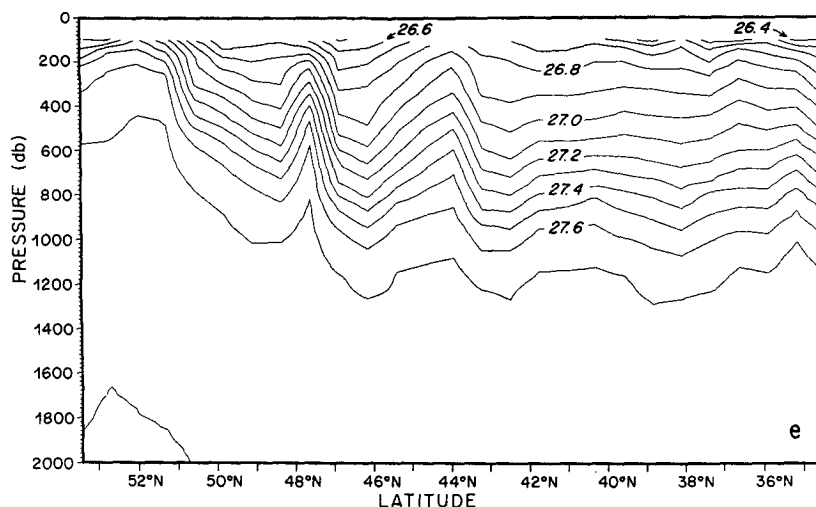
FIG. 7. (Continued)

in the center of the density front the slopes for the isobaric-averaged field are steeper than those for the isopycnal-averaged ones, 2.7 db/km compared to 2.0 db/km. Integrating over the upper 1000 db, this difference in slope is equivalent to an increase of 10 cms^{-1} surface velocity for the isobaric-averaged field over the approximate 30 cms^{-1} velocity that one obtains for the isopycnal-averaged field. Thus, the isobaric fields would have a higher maximum surface velocity in the Gulf Stream, which in turn would imply a possible significant change in property flux estimates, such as heat flux.

The difference between the two fields (Figs. 8b and c) is shown in Fig. 8d. The dominant feature in this difference field is the vertical dipole centered on the Gulf Stream axis, which indicates that isobaric averaging produces lighter potential densities in the upper thermocline and heavier densities in the middle to lower thermocline. The slight horizontal shift between the two centers in the dipole is the result of the lower isopycnals deepening on the southern side of the front while the shallower ones shoal on the northern side. In other words, the maximum anomaly is centered where the isopycnal slope is the strongest. The dipole pattern can be explained by reexamining the potential density section (Fig. 8a). For a 200-km envelope that spans the sloping front of the Gulf Stream and that is unchanging with depth, an average along an isobar in the upper water column will favor lighter waters (because the front is shifted toward the dense water side), while an average in the middle to lower thermocline will favor denser waters (because the front is shifted toward the lighter water side). Thus, a potential density calculated from isobaric-averaged temperatures and salinities will be lighter (denser) than the isopycnal-averaged potential density for the upper (mid to lower) thermocline waters. The magnitude of this potential

density anomaly (on the order of 0.2 σ_θ units) is sufficient to vertically displace the isopycnal surface approximately 100 to 200 m and is sufficient to create a shear difference of approximately 10–20 cms^{-1} over 1000-m depth, as noted above. Given that the velocities for the *mean* Gulf Stream at 55°W (in geographic coordinates) drop from approximately 50 to 10 cms^{-1} over 1000-m depth (Richardson 1985), such shear anomalies would have a sizable impact.

b. Impact on usages of averaged data

Beyond the basic analyses discussed above, averaged data has a host of other uses. A prevalent usage has been with inverse models, where the averaged data along with assumed dynamics are used to deduce an estimate of the mean circulation. One need only to consider the isolated lozenge of warm salty water in Fig. 1c to appreciate how such an anomaly could contaminate these inversions. Because such a closed pool of water cannot be maintained by horizontal processes (advection or mixing), more than likely a spurious vertical process would result from an inversion using this data. Diapycnal velocities and mixing coefficients, which are not particularly robust quantities to begin with, would be especially sensitive to such anomalies. Use of averaged data in model inversions illustrates perhaps the most damaging consequence of using averaged data: that spurious circulations would be needed to explain features created by the averaging process alone. Unfortunately, we cannot think of an inversion technique that would not be susceptible to these artifacts. To a lesser degree, it is anticipated that forward models would be sensitive to these averaging artifacts if they use averaged data for initialization and/or assimilation.

Averaged data has also been used recently to illustrate differences between isopycnal surfaces and neutral
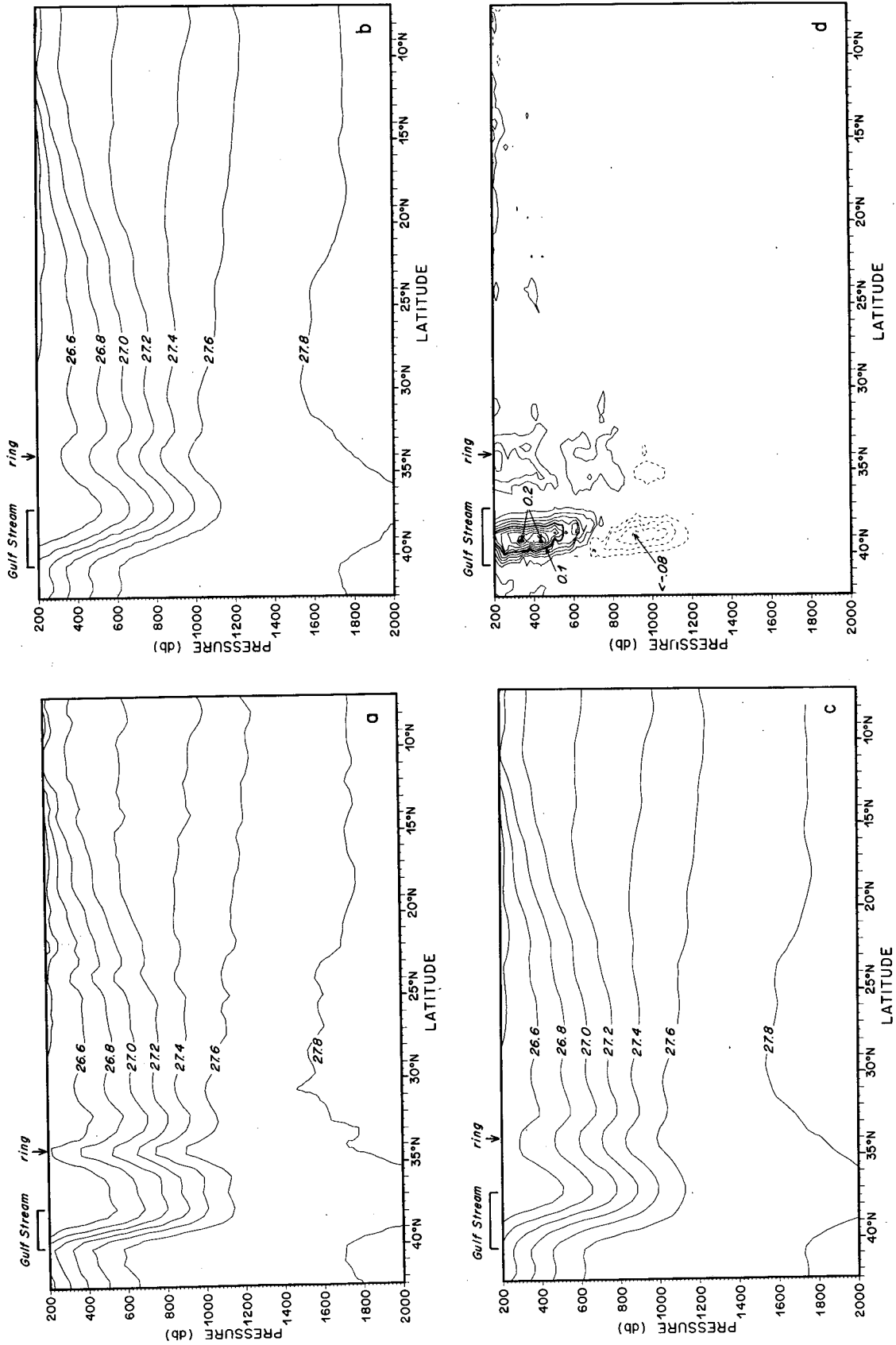
FIG. 8. Potential density for the 53°W section using (a) unaveraged data, (b) isopycnal-averaged data, and (c) isobaric-averaged data. Contour interval is 0.2 σ_t units for each plot. (d) A plot of the difference between the potential density calculated from the isopycnal-averaged data and that calculated from the isobaric-averaged data ($\sigma_{isopycnal\ averaged} - \sigma_{isobaric\ averaged}$). Contour interval is 0.02 σ_t units, and the zero contour is not included.

surfaces (McDougall 1987a). A map of the potential density difference (McDougall 1987a, Fig. 6d) between an isopycnal and a neutral surface in the North Atlantic basin shows that the surfaces diverge as the paths cross the basin such that differences on the order of 0.1 (σ_θ units) accrue. As was shown in the last section, in the vicinity of sloping isopycnals, isobaric averaging can produce potential density anomalies on the order of 0.1 (σ_θ units). Thus, errors of this magnitude can dominate the differences between neutral and potential density surfaces when isobaric-averaged data is used. Therefore, it is suggested, that a pressure-averaged database is unsuitable to detect differences between isopycnals and neutral surfaces. (We note that in the present analysis we found negligible differences between neutral surfaces and isopycnals as long as the reference pressure for the isopycnals was close to the observed pressure of that surface.)

Another effect of isobaric averaging that could cause difficulties is the change of the slope and curvature of the θ–S relation (Fig. 4b). Schmitt (1981, 1990) has drawn attention to the fact that the slightly curved θ–S relation of the NACW is well represented by a curve of constant density ratio, which is defined as the product of the θ–S slope and the ratio of the thermal expansion coefficient to the haline contraction coefficient. The artifact due to isobaric averaging in the Gulf Stream causes a slight rotation of the θ–S relation toward smaller slopes, and thus would tend to alter the apparent density ratio. The θ–S relation curvature also enters in mixing processes described by McDougall (1987b). For example, in the determination of turbulent vertical diffusivity's contribution to temperature and salinity changes on neutral surfaces, the curvature appears as a multiplicative coefficient of the diffusivity. The flattening of the curvature caused by the averaging artifacts will thus reduce the apparent contribution of vertical diffusivity to heat and salt fluxes along those surfaces.

c. Advantages of isopycnal averaging

There are two main reasons for preferring isopycnal averaging. The first is simply the recognition that because the ocean mixes primarily along isopycnals, averaging along these surfaces is equivalent to mixing by oceanic processes. The same cannot be said for averaging along pressure surfaces in the presence of a meandering potential density front, for its action is to average water characteristics from well-separated isopycnals, effectively acting as an intensified vertical mixing. The isolated lozenge and the warm tongue extending along the axis of the North Atlantic Current (Fig. 1c) represent the result of this artificial diapycnal mixing. A second advantage of averaging on potential density surfaces is that it retains, to a certain extent, an aspect of stream-coordinate averaging. Because the smoothing effect of meandering is removed, such an

averaging preserves, to a large degree, the strong frontal gradients of the instantaneous stream. With meandering included an unrealizable mean Gulf Stream is obtained. Use of stream coordinates has been ideal for studying the Gulf Stream in isolation, but it is clearly inadequate when a mean Gulf Stream needs in be placed in geographic context. Although isopycnal averaging smooths the frontal gradients, a degree of stream coordinate averaging can be recovered because such averaging *does* preserve the synoptic water mass properties. Conversely, we would argue that isobaric averaging produces not only unrealizable frontal gradients but also unrealizable and *misrepresentative* water properties. A case for misrepresentation can be made with the warm lozenge in the Levitus potential temperature map (Fig. 1c). The temperature–salinity characteristics of the water within the lozenge (9.0°–9.2°C and 35.3–35.4 psu) are not within the bounds of known water mass characteristics for the western North Atlantic as given by the Wright and Worthington volumetric census (1970). By contrast, the temperature–salinity characteristics of the water in the LOC field (8.2°C and 35.1 psu) lie within the observed temperature–salinity range.

5. Conclusions

Averaging on pressure surfaces creates anomalous θ–S characteristics in the vicinity of sloping isopycnals. It has been shown that the artifacts are of sufficient strength to affect interpretations of water mass variation and of circulation patterns. Given that the two criteria for the effect to occur (sloping isopycnals and curvature in the θ–S relationship) are fairly ubiquitous, it is suggested that these anomalous anomalies are not restricted to fronts in the North Atlantic, but rather would be found throughout the global ocean. Further generalizing our work we would add that isobaric averaging will affect *any* nonlinear water mass relation (e.g., σ–O_2 and σ–potential vorticity). Finally, based on the results presented in this paper it is suggested that climatological hydrographic data be averaged on potential density surfaces in order to prevent averaging anomalies and to preserve, to a large extent, synoptic water mass characteristics.

REFERENCES

Armi, L., and N. A. Bray, 1982: A standard analytic curve of potential temperature versus salinity for the western North Atlantic. *J. Phys. Oceanogr.*, **12**, 384–387.

Cornillion, P., 1986: The effect of the New England Seamounts on Gulf Stream meandering as observed from satellite IR imagery. *J. Phys. Oceanogr.,* **16,** 386–389.

Fuglister, F. C., 1963: Gulf Stream '60. *Progress in Oceanography,* Vol. 1, Pergamon, 265–373.

Iselin, C. O'D., 1936: A study of the circulation of the western North Atlantic. *Pap. Phys. Oceanogr.,* **4**(4), 101 pp.

Johns, E., D. R. Watts, and H. T. Rossby, 1989: A test of geostrophy in the Gulf Stream. *J. Geophys. Res.,* **94**(C3), 3211–3222.

Knapp, G. P., and H. M. Stommel, 1985: Hydrographic data from R/V OCEANUS Cruise 133, leg VII. Woods Hole Oceanographic Institution Tech. Rep., WHOI-85-38, 107 pp.

Levitus, S., 1982: *Climatological Atlas of the World Ocean.* U.S. Gov. Printing Office, Washington, DC, NOAA Prof. Paper No. 13, 173 pp.

Lozier, M. S., W. B. Owens, and R. G. Curry, 1994: The climatology of the North Atlantic. *Progress in Oceanography,* in press.

McCartney, M. S., 1992: Recirculating components to the deep boundary current of the northern North Atlantic. *Progress in Oceanography,* Vol. 29, Pergamon, 283–383.

——, L. V. Worthington, and M. E. Raymer, 1980: Anomalous water mass distributions at 55 degrees W in the North Atlantic in 1977. *J. Mar. Res.,* **38,** 147–172.

McDougall, T. J., 1987a: Neutral surfaces. *J. Phys. Oceanogr.,* **17,** 1950–1964.

——, 1987b: Thermobaricity, cabbeling and water mass conversion. *J. Geophys. Res.,* **92,** 5448–5464.

Richardson, P. L., 1985: Average velocity and transport of the Gulf Stream near 55W. *J. Mar. Res.,* **43,** 83–111.

Schmitt, R. W., 1981: Form of the temperature–salinity relationship in the central water: Evidence for double-diffusive mixing. *J. Phys. Oceanogr.,* **11,** 1015–1026.

——, 1990: On the density ratio balance in the central water. *J. Phys. Oceanogr.,* **19,** 1208–1221.

Worthington, L. V., 1976: On the North Atlantic circulation. *The Johns Hopkins Oceanographic Studies,* No. 6, 110 pp.

——, and W. G. Metcalf, 1961: The relationship between potential temperature and salinity in deep Atlantic water. *Rapp. P.-V. Reun. Cons. Int. Explor. Mer.,* **149,** 122–128.

Wright, W. R., and L. V. Worthington, 1970: The water masses of the North Atlantic Ocean: A volumetric census of temperature and salinity. *Serial Atlas of the Marine Environment,* Folio 19, Amer. Geogr. Soc., 8 pp. and 7 plates.